

This is the accepted manuscript made available via CHORUS. The article has been published as:

Driven-dissipative Ising model: Mean-field solution

G. Goldstein, C. Aron, and C. Chamon

Phys. Rev. B **92**, 174418 — Published 23 November 2015

DOI: [10.1103/PhysRevB.92.174418](https://doi.org/10.1103/PhysRevB.92.174418)

Driven-dissipative Ising model: mean-field solution

G. Goldstein,¹ C. Aron,^{2,3} and C. Chamon⁴

¹*Department of Physics, Rutgers University, Piscataway, New Jersey 08854, USA*

²*Department of Electrical Engineering, Princeton University, Princeton, New Jersey 08544, USA*

³*Instituut voor Theoretische Fysica, KU Leuven, Belgium*

⁴*Department of Physics, Boston University, Boston, Massachusetts 02215, USA*

We study the fate of the Ising model and its universal properties when driven by a rapid periodic drive and weakly coupled to a bath at equilibrium. The far-from-equilibrium steady-state regime is accessed by means of a Floquet mean-field approach. We show that, depending on the details of the bath, the drive can strongly renormalize the critical temperature to higher temperatures, modify the critical exponents, or even change the nature of the phase transition from second to first order after the emergence of a tricritical point. Moreover, by judiciously selecting the frequency of the field and by engineering the spectrum of the bath, one can drive a ferromagnetic Hamiltonian to an antiferromagnetically ordered phase and *vice-versa*.

PACS numbers:

The Ising model is undoubtedly the most studied model of statistical mechanics. Besides its equilibrium properties, its coarsening dynamics following a temperature quench from the paramagnetic to the ordered phase is also quite well understood [1, 2], even in the presence of weak disorder [3–5]. Taking into account the dissipative mechanisms due to the inevitable coupling of the spin system to an environment has been successful in the description of important many-body phenomena based on the Ising model such as the decay of metastable phases [8–13], hysteretic responses [15–17] and magnetization switching in mesoscale ferromagnets [18, 19]. As it is becoming clear these days that driven-dissipative physics, *i.e.* the balancing of non-equilibrium conditions and dissipative mechanisms [20], is a promising route to achieve a new type of control over matter, a burning question arises: can the Ising model be driven to non-equilibrium steady states (NESS) with enhanced or even novel properties?

This question has been approached in the context of slowly oscillating drives (magnetic fields or electrochemical potentials) by means of Monte-Carlo simulations [14–17, 27–29], mean-field treatment [21–26], or other analytical techniques [30–33]. One of the key results is the existence of a so-called dynamical phase transition, where the cycle-averaged magnetization becomes non-zero in a singular fashion. This has recently been supported by experimental evidence in the dynamics of thin ferromagnetic films [34].

In this Letter, we focus on the Ising model driven by a rapidly oscillating magnetic field $h \cos(\omega t)$. We depart from the usual Floquet engineering of many-body states (the Floquet Hamiltonian for this system is simply the unperturbed Ising model and as such shows no new interesting phases) which is mostly directed towards cold-atomic systems [35], by including a dissipative mechanism, namely by weakly coupling the system to an external bath at equilibrium. We access the non-equilibrium steady states by means of a Floquet mean-field approach.

We derive the mean-field self-consistent equation for the magnetization and use it to derive the non-equilibrium phase diagram. Whenever analytical solutions are beyond reach, we complete the picture with numerical results. Our main results are to show how the combination of drive (*i.e.* h and ω) and dissipation (mostly the low-energy spectrum of the bath) can be used to increase the critical temperature T_c , to modify the critical exponent β_T , as well as to change the order of the phase transition. Additionally, we show that the drive can, in the presence of carefully selected baths, convert a ferromagnetically ordered system to an antiferromagnetic order, and *vice versa*.

I. MODEL

The total Hamiltonian is composed of the system, the bath and the system-bath Hamiltonians, $H(t) = H_S(t) + H_B + H_{SB}$ with (we set $\hbar = k_B = 1$)

$$H_S(t) = -J \sum_{\langle ij \rangle} \sigma_i^z \sigma_j^z - h \cos(\omega t) \sum_i \sigma_i^z, \quad (1a)$$

$$H_B = \sum_{i,\alpha} \omega_\alpha b_{i,\alpha}^\dagger b_{i,\alpha}, \quad (1b)$$

$$H_{SB} = \sum_{i,\alpha} t_\alpha \sigma_i^x (b_{i,\alpha} + b_{i,\alpha}^\dagger). \quad (1c)$$

The $S = 1/2$ spins, represented at each site i of the bipartite lattice by the usual Pauli operators $\sigma_i^{x,y,z}$, are interacting through a nearest-neighbor interaction J . h is the strength of the periodic drive with frequency $\omega \equiv 2\pi/\tau$ (we choose $\omega \geq 0$). Equilibrium conditions are recovered for $h = 0$ or $\omega = 0$.

The environment is composed of local baths expressed in terms of a collection of non-interacting bosonic modes labelled by α , with energy ω_α and with creation and annihilation operators $b_{i,\alpha}^\dagger$ and $b_{i,\alpha}$. Each bath is in equilib-

rium at temperature $T \equiv 1/\beta$ and we assume it is a “good bath”, *i.e.* it has a very large number of degrees of freedom and it remains in thermal equilibrium. Below, we replace \sum_α by $\int d\epsilon \rho(\epsilon)$ where $\rho(\epsilon)$ is the bath density of states. Without loss of generality, the chemical potential is set to 0 and $\rho(\epsilon < 0) = 0$. t_α sets the strength of the spin-bath interactions. After integrating out the bath degrees of freedom, the bath will enter the reduced problem *via* the hybridization function $\nu(\epsilon) \equiv |t(\epsilon)|^2 \rho(\epsilon)$. The low-energy behavior of the hybridization $\nu(\epsilon) \underset{0 < \epsilon \rightarrow 0}{\sim} \epsilon^{1+s}$

characterizes whether the bath is Ohmic ($s = 0$), sub-Ohmic ($s < 0$), or super-Ohmic ($s > 0$). We do not consider additional system-bath coupling terms such as $\sigma_i^{y,z} (b_{i,\alpha} + b_{i,\alpha}^\dagger)$ because they do not induce any qualitative change in the non-equilibrium dynamics.

We stress that it is the system-bath coupling which generates the quantum dynamics, *via* the non-commutation of σ_i^x with the rest of the model. In the absence of a finite coupling to the environment, our drive would indeed have a rather marginal impact since $[\sigma_i^z, H(t)] = 0$ at all times, implying that all the degrees of freedom would be conserved quantities. It is therefore the interplay between the bath-induced spin flips and the magnetic-field driven time-dependent phases of the wave vectors [see *e.g.* Eq. (3) below] which will result in non-trivial dynamics.

II. NON-EQUILIBRIUM STEADY-STATE DESCRIPTION

A. Floquet mean-field picture

The time-dependent mean-field Hamiltonian corresponding to $H(t)$ in Eq. (1) is the one of a single spin coupled to its local bath, and reads $\bar{H}(t) = \bar{H}_S(t) + \bar{H}_B + \bar{H}_{SB}$ with

$$\bar{H}_S(t) = -zJ\varphi(t)\sigma^z - h\sigma^z \cos(\omega t), \quad (2a)$$

$$\bar{H}_B = \sum_\alpha \omega_\alpha b_\alpha^\dagger b_\alpha, \quad (2b)$$

$$\bar{H}_{SB} = \sum_\alpha t_\alpha \sigma^x (b_\alpha + b_\alpha^\dagger). \quad (2c)$$

Here, $\varphi(t)$ is the expectation value of $\sigma^z(t)$ which serves as the order parameter, and z is the coordination number of the bipartite lattice (this approach becomes exact in the limit of infinite dimensions $z \rightarrow \infty$). When the coupling to the bath is weak (see the discussion below), the spin subsystem can be seen as quasi-isolated during many periods of the drive. There, the Floquet theorem states that the instantaneous eigenstates of the time-periodic Hamiltonian $\bar{H}_S(t)$ can be written in the form $|\psi_\alpha(t)\rangle = e^{-iE_\alpha t} |\psi_\alpha^P(t)\rangle$ where E_α is a so-called Floquet quasi-energy and $|\psi_\alpha^P(t)\rangle$ is periodic: $|\psi_\alpha^P(t + \tau)\rangle =$

$|\psi_\alpha^P(t)\rangle$. Owing to the fact that σ^z is a conserved quantity, we may choose our Floquet eigenstates to simultaneously diagonalize σ^z . Note that this also implies that $\varphi(t)$ is a constant (at least between two events induced by the weakly-coupled bath). Altogether, the instantaneous eigenstates of $\bar{H}_S(t)$ are simply given by

$$|\uparrow(t)\rangle = e^{+i[zJ\varphi t + \frac{h}{\omega} \sin(\omega t)]} |\uparrow\rangle = e^{-i\epsilon_\uparrow t} |\uparrow^P(t)\rangle, \quad (3)$$

$$|\downarrow(t)\rangle = e^{-i[zJ\varphi t + \frac{h}{\omega} \sin(\omega t)]} |\downarrow\rangle = e^{-i\epsilon_\downarrow t} |\downarrow^P(t)\rangle, \quad (4)$$

from which one identifies the Floquet quasi-energies and the periodic states, reading

$$\epsilon_\uparrow \equiv -zJ\varphi, \quad |\uparrow^P(t)\rangle = \sum_n J_n(h/\omega) e^{-in\omega t} |\uparrow\rangle, \quad (5)$$

$$\epsilon_\downarrow \equiv zJ\varphi, \quad |\downarrow^P(t)\rangle = \sum_n J_n(h/\omega) e^{+in\omega t} |\downarrow\rangle, \quad (6)$$

where J_n are the Bessel functions of the first kind.

B. Transition rates

The bath induces incoherent transitions between the Floquet states. Assuming that the bath correlation functions relax in a time much shorter than the driving period (Markov approximation), the transition rate $R_{\uparrow\downarrow}$ from $|\uparrow\rangle$ to $|\downarrow\rangle$ can be obtained by means of a Floquet-Fermi golden rule [6, 7]:

$$R_{\uparrow\downarrow}(\varphi) = 2\pi \sum_{m \in \mathbb{Z}} |A_{\uparrow\downarrow}^m|^2 g(\epsilon_\uparrow - \epsilon_\downarrow + m\omega), \quad (7)$$

with $g(\epsilon) \equiv \nu(\epsilon)[1 + n_B(\epsilon)] + \nu(-\epsilon)n_B(-\epsilon)$ where the Bose-Einstein distribution $n_B(\epsilon) \equiv 1/(e^{\beta\epsilon} - 1)$ and

$$A_{\uparrow\downarrow}^m \equiv \int_0^\tau \frac{dt}{\tau} \langle \downarrow^P(t) | \sigma^x | \uparrow^P(t) \rangle e^{im\omega t} = J_m(2h/\omega). \quad (8)$$

A similar expression can be obtained for the rate $R_{\downarrow\uparrow}(\varphi)$ with $A_{\uparrow\downarrow}^m = A_{\downarrow\uparrow}^{-m}$. Importantly, these rates do not satisfy detailed balance, contrary to equilibrium dynamics this would hold even in situations in which the spin relaxation is much faster than the drive. Note that the integration over the degrees of freedom of the bath also contributes to a small renormalization of the spin Hamiltonian (so-called Lamb-shift) that we neglect.

C. Steady-state populations

We stress that the previous analysis is valid only in the case when the bath is *weakly* coupled to the system, *i.e.* the rate at which it induces spin flips is much smaller than the frequency of the drive: $R_{\uparrow\downarrow}, R_{\downarrow\uparrow} \ll \omega$. Under these conditions, $\varphi(t)$ is indeed constant over many periods of the drive and a time-translational invariant non-equilibrium steady state can settle. Once it is reached,

the probabilities of being in the $|\uparrow\rangle$ and $|\downarrow\rangle$ states are simply given by

$$P_{\uparrow}^{\text{NESS}} = \frac{1}{1 + R_{\uparrow\downarrow}/R_{\downarrow\uparrow}} \text{ and } P_{\downarrow}^{\text{NESS}} = 1 - P_{\uparrow}^{\text{NESS}}. \quad (9)$$

D. Self-consistency condition

The probabilities in Eq. (9) allow us to compute the steady-state average magnetization as $|\varphi| = |P_{\uparrow}^{\text{NESS}} -$

$P_{\downarrow}^{\text{NESS}}|$. Therefore, we obtain the self-consistency condition for the mean-field order parameter

$$\pm \varphi = \frac{R_{\downarrow\uparrow}(\varphi) - R_{\uparrow\downarrow}(\varphi)}{R_{\downarrow\uparrow}(\varphi) + R_{\uparrow\downarrow}(\varphi)}. \quad (10)$$

Here, the $+$ sign corresponds to a ferromagnetic order while the $-$ sign corresponds to an antiferromagnetic order. Making use of the expression for the rates given in Eq. (7), we obtain

$$R_{\downarrow\uparrow}(\varphi) - R_{\uparrow\downarrow}(\varphi) = 2\pi |J_0(2h/\omega)|^2 \nu(|2zJ\varphi|) \text{sgn}(J\varphi) + 2\pi \sum_{n>0} \sum_{a,b=\pm} |J_n(2h/\omega)|^2 b \nu(an\omega + 2bzJ\varphi), \quad (11a)$$

$$R_{\downarrow\uparrow}(\varphi) + R_{\uparrow\downarrow}(\varphi) = 2\pi |J_0(2h/\omega)|^2 \nu(|2zJ\varphi|) \coth(\beta|zJ\varphi|) + 2\pi \sum_{n>0} \sum_{a,b=\pm} |J_n(2h/\omega)|^2 \nu(an\omega + 2bzJ\varphi) \coth(\beta(an\omega + 2bzJ\varphi)/2). \quad (11b)$$

In case the ac drive is switched off, $h = 0$, one naturally recovers

$$\pm \varphi = \frac{R_{\downarrow\uparrow}(\varphi) - R_{\uparrow\downarrow}(\varphi)}{R_{\downarrow\uparrow}(\varphi) + R_{\uparrow\downarrow}(\varphi)} \xrightarrow{h=0} \tanh \beta z J \varphi, \quad (12)$$

which is the familiar self-consistent condition for the Ising model in thermal equilibrium. In this case, it is well known that there is a second-order phase transition at the critical temperature $T_c^{\text{eq}} = zJ$, below which ferromagnetic solutions are possible for $J > 0$ and antiferromagnetic ones for $J < 0$.

III. NON-EQUILIBRIUM STEADY-STATE PHASE DIAGRAM

The self-consistency equation (10) together with Eqs. (11a) and (11b) allow us to explore the complete mean-field phase diagram far from the equilibrium regime. Let us first investigate the fate of the well-known second-order phase transition in this out-of-equilibrium context. In order to access its locus in parameter space, we expand and solve Eq. (10) around $\varphi = 0$. To start let's assume a power law density of states for the bath more precisely using the low-energy parametrization of the bath hybridization $\nu(\epsilon) \underset{\epsilon \rightarrow 0^+}{\simeq} \eta \epsilon^{1+s}$, we obtain

$$\pm \varphi = \frac{R_{\downarrow\uparrow}(\varphi) - R_{\uparrow\downarrow}(\varphi)}{R_{\downarrow\uparrow}(\varphi) + R_{\uparrow\downarrow}(\varphi)} = \beta z J \varphi \frac{K |2zJ\varphi|^s + A}{K |2zJ\varphi|^s + B}, \quad (13)$$

where

$$\begin{aligned} K &\equiv \eta |J_0(2h/\omega)|^2, \\ A &\equiv 2 \sum_{n>0} |J_n(2h/\omega)|^2 \nu'(n\omega), \\ B(T) &\equiv \beta \sum_{n>0} \left| J_n \left(\frac{2h}{\omega} \right) \right|^2 \nu(n\omega) \coth \left(\frac{\beta n\omega}{2} \right). \end{aligned}$$

Besides the trivial solution $\varphi = 0$, the self-consistent mean-field equation (13) admits non-zero solutions

$$|\varphi| = \frac{1}{2T_c^{\text{eq}}} \left[\frac{B(T)}{K} \frac{\pm \text{sgn}(J) [A/B(T)] T_c^{\text{eq}} - T}{T \mp \text{sgn}(J) T_c^{\text{eq}}} \right]^{1/s}. \quad (14)$$

Equation (14) above is quite rich and its analysis below will tell us about 1) the critical temperature, 2) the nature of the ordered phase (and the stability of the non-trivial solutions), 3) the critical exponent, and 4) the nature of the phase transition.

Note that φ in Eq. (14) must vanish continuously when crossing a second-order phase transition. For a bath with a sub-Ohmic low-energy behavior, $-1 \leq s < 0$, this implies that the corresponding critical temperature, T_c , is identical to the equilibrium case: $T_c = T_c^{\text{eq}}$. Thereafter, unless stated otherwise, we shall focus on baths with a super-Ohmic low-energy behavior, $s > 0$. In this case, the critical temperature is the non-trivial solution of $T_c = \pm \text{sgn}(J) [A/B(T_c)] T_c^{\text{eq}}$. Before solving explicitly for T_c , one can already remark that T_c must be larger than T_c^{eq} so that the numerator and denominator of Eq. (14) have the same sign for $T_c^{\text{eq}} < T < T_c$, ensuring a well-defined non-zero magnetization solution in that temperature range.

Let us now solve for T_c for a more general bath density of states by considering the case when $h \ll \omega$, for which only the $n = 1$ mode contributes significantly (because of the stronger power decay of the Bessel functions for larger n 's). In this case, the critical temperature T_c is determined by

$$\tanh\left(\frac{\omega}{2T_c}\right) = \pm \text{sgn}(J) \frac{1}{2T_c^{\text{eq}}} \frac{\nu(\omega)}{\nu'(\omega)}. \quad (15)$$

Note that Eq. (15) has a finite solution only if the norm of the right-hand side is smaller than unity.

Importantly, when $\nu'(\omega) > 0$, the type of order is dictated by the sign of J in the ordinary way: $J > 0$ for a ferromagnet, $J < 0$ for an anti-ferromagnet. However, it is noteworthy that driving can turn a ferromagnet into an anti-ferromagnet and vice-versa when $\nu'(\omega) < 0$. The choice of sign in Eq. (15) that yields a positive transition in this case is the *opposite* of the common Ising model: here when $J > 0$, there is an *anti-ferromagnetic* solution, and when $J < 0$, there is a *ferromagnetic* solution.

Eq. (15) can be solved analytically when the right-hand side of the equation is much smaller than unity, $\nu(\omega)/|\nu'(\omega)| \ll T_c^{\text{eq}}$, yielding the critical temperature

$$T_c \approx T_c^{\text{eq}} |\omega \nu'(\omega)| / \nu(\omega). \quad (16)$$

Eq. (16) transparently elucidates that by judiciously choosing the driving frequency or engineering the bath, or both, one can achieve a rather large critical temperatures T_c , much larger than the one for the undriven system, T_c^{eq} . To exemplify this point, let us assume that the low-energy behavior of the hybridization $\nu(\epsilon) \sim \epsilon^{1+s}$ ($s > 0$) holds up to the scale ω . This yields $T_c \approx (1+s)T_c^{\text{eq}} > T_c^{\text{eq}}$. See also Fig. 1 where we plotted the magnetization as a function of the temperature for different drive strengths. In the temperature range $T_c^{\text{eq}} < T < T_c$, it can be seen from Eq. (14) that the drive is responsible for a finite magnetization on the order of $|\varphi| \sim (h/\omega)^{2/s} \omega/zJ$. This explains why in the limit $0 \leftarrow h \ll \omega$ the equilibrium results are recovered. In the Appendix A, we show the stability of this non-trivial mean-field solution below T_c . In Fig. 2, we summarized the non-equilibrium phase diagram in the temperature-drive plane by numerically solving for the critical temperatures in all the regimes of h and ω . Beyond the super-Ohmic case, Eq. (15) suggests that one can engineer very high critical temperatures by using the edges of the bath spectrum to realize very large $|\nu'(\omega)|$ or by embedding the spins in optical cavities with a finely tunable sharply peaked spectrum.

Equation (14) also readily provides the mean-field critical exponent for the order parameter as function of temperature, $\beta_T = 1/s$, to be contrasted with the undriven case where the mean-field exponent is $\beta_T^{\text{eq}} = 1/2$. This means that, even at the mean-field level, driving changes the nature the phase transition.

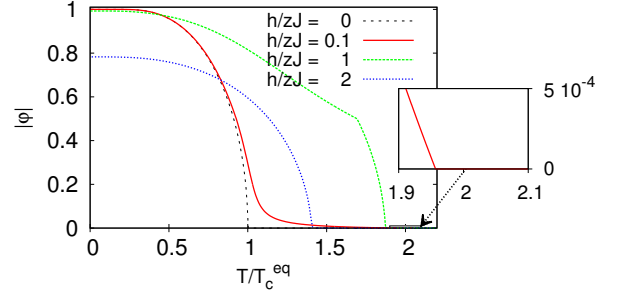


Figure 1: (color online) Mean-field magnetization $|\varphi|$ as a function of the temperature T of the bath (super-Ohmic case, $s = 1$) for different values of the drive h given by the key: $h = 0$ (equilibrium), $h \ll \omega$, $h \sim \omega$ and $h > \omega$. The driving frequency is chosen to be $\omega = zJ = T_c^{\text{eq}}$. The critical temperature for $h \ll \omega$, $T_c = (1+s)T_c^{\text{eq}}$, is computed exactly in Eq. (16). In the temperature range $T_c^{\text{eq}} < T < T_c$, $|\varphi| \sim (h/\omega)^{2/s} \omega/zJ$.

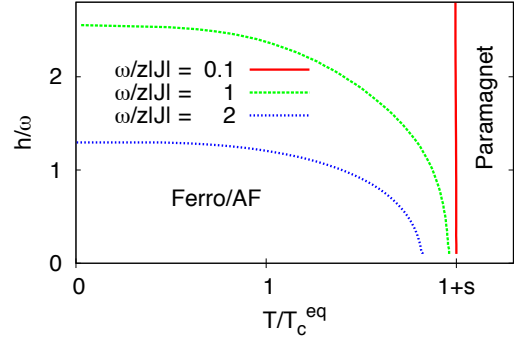


Figure 2: Non-equilibrium phase diagram in the drive vs temperature plane for different values of ω given in the key, for the case of the super-Ohmic bath ($s = 1$).

Finally, Eq. (14) predicts a diverging magnetization at $T = T_c^{\text{eq}}$. Although it was derived under the assumption that φ is small, this suggests that the original self-consistency Eq. (10) may have non-trivial solutions $\varphi \neq 0$ which are not connected continuously to $\varphi = 0$ and signaling the presence of a first-order phase transition. For example, in the case of baths with a sub-Ohmic low-energy behavior ($-1 \leq s < 0$), the denominator of Eq. (10) given in Eq. (11b) has $1/(\varphi - \varphi_n)$ divergences located at every $\varphi_n \equiv n\omega/2zJ$ for $n = 1 \dots \lfloor 2zJ/\omega \rfloor$. In turn, this implies the presence of a collection of non-trivial solutions of the self-consistent Eq. (10) close to these φ_n 's. For baths with a super-Ohmic low-energy behavior, the denominator Eq. (11b) is well-behaved and we investigate the possibility of a first-order phase transition by solving Eq. (10) numerically. In Fig. 3, we show

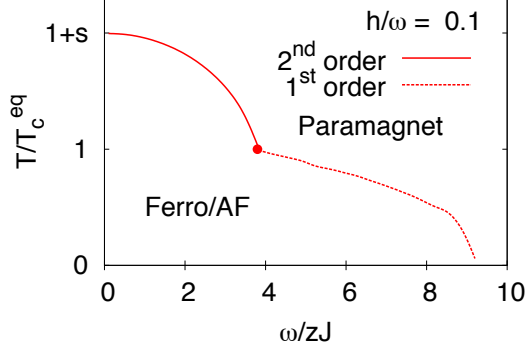


Figure 3: Non-equilibrium phase diagram in temperature vs drive frequency for fixed $h/\omega = 0.1$ and for the case of a super-Ohmic bath ($s = 1$). The red circle indicates the location of the tricritical point separating a second order (plain) line from first-order (dashed) line.

the non-equilibrium phase diagram in the T - ω plane for a fixed h/ω . Starting from small drive frequencies, the line of second-order phase transitions reaches a tricritical point located at $(\omega^*(h/\omega), T_c^* = T_c^{\text{eq}})$ and turns into a line of first-order transitions for larger ω .

IV. DISCUSSION

Besides the demonstration that driven-dissipative conditions can strongly reshape the phase diagram of the Ising model, this study allows us to shine a new light on the fate of the universal properties of this model and, by extension, other similar models when driven to non-equilibrium steady states. When the drive is finite, we have found that the critical exponents (and the critical temperature) are strongly dependent on the details of the bath, thus losing much of their universality. However, a certain universality still subsists in the fact that only the low-energy behavior of the bath determines those new critical exponents. In the Appendix B, we consolidate the validity of our mean-field results in finite dimensions by means of a numerical Monte Carlo approach.

This work has been supported by the Rutgers CMT fellowship (G.G.), the NSF grant DMR-115181 (C.A.), and the DOE Grant DEF-06ER46316 (C.C.).

Appendix A: Stability of the mean-field solutions

Here we check whether the non-zero mean-field solutions in Eq. (19) are stable. We start with a Master Equation for the probabilities P_\uparrow and P_\downarrow in terms of the

rates $R_{\downarrow\uparrow}$ and $R_{\uparrow\downarrow}$:

$$\begin{aligned}\dot{P}_\uparrow &= -R_{\uparrow\downarrow}P_\uparrow + R_{\downarrow\uparrow}P_\downarrow \\ \dot{P}_\downarrow &= +R_{\uparrow\downarrow}P_\uparrow - R_{\downarrow\uparrow}P_\downarrow.\end{aligned}$$

Using $P_\uparrow = (1 \pm \varphi)/2$ and $P_\downarrow = (1 \mp \varphi)/2$ for the ferromagnetic and anti-ferromagnetic cases, respectively, yields

$$\pm \dot{\varphi} = [R_{\downarrow\uparrow}(\varphi) - R_{\uparrow\downarrow}(\varphi)] - [R_{\downarrow\uparrow}(\varphi) + R_{\uparrow\downarrow}(\varphi)] (\pm \varphi)$$

or, equivalently,

$$\dot{\varphi} = -[R_{\downarrow\uparrow}(\varphi) + R_{\uparrow\downarrow}(\varphi)] \left\{ \varphi \mp \frac{R_{\downarrow\uparrow}(\varphi) - R_{\uparrow\downarrow}(\varphi)}{R_{\downarrow\uparrow}(\varphi) + R_{\uparrow\downarrow}(\varphi)} \right\}.$$

The quantity in curly brackets vanishes at the stationary point, and gives precisely the condition in Eq. (14). Let $\bar{\varphi}$ be this stationary point solution. To consider the stability of fluctuations, we expand $\varphi = \bar{\varphi} + \delta\varphi$. The expansion of the terms in curly brackets start at order $\delta\varphi$ (because $\bar{\varphi}$ is where it vanishes); so to lowest order, the term in square brackets does not need to be expanded. The linearized stability equation becomes

$$\delta \dot{\varphi} = -[R_{\downarrow\uparrow}(\bar{\varphi}) + R_{\uparrow\downarrow}(\bar{\varphi})] [1 \mp C(\bar{\varphi})] \delta\varphi,$$

where

$$C(\bar{\varphi}) = \frac{d}{d\varphi} \left(\frac{R_{\downarrow\uparrow}(\varphi) - R_{\uparrow\downarrow}(\varphi)}{R_{\downarrow\uparrow}(\varphi) + R_{\uparrow\downarrow}(\varphi)} \right) \Big|_{\bar{\varphi}}.$$

Notice that $R_{\downarrow\uparrow}(\bar{\varphi}) + R_{\uparrow\downarrow}(\bar{\varphi}) > 0$, so the stability of the solution rests upon whether $[1 \mp C(\bar{\varphi})] > 0$.

Using Eq. (18), we find

$$\begin{aligned}1 \mp C(\bar{\varphi}) &= \mp \beta z J \frac{d}{d\varphi} \frac{K |2zJ\varphi|^s + A}{K |2zJ\varphi|^s + B} \Big|_{\bar{\varphi}} \\ &= \mp \beta z J (A - B) \left[\frac{d}{d\varphi} \frac{1}{K |2zJ\varphi|^s + B} \Big|_{\bar{\varphi}} \right].\end{aligned}$$

The quantity in the square bracket above is always negative. Therefore, the sign of $1 \mp C(\bar{\varphi})$ is that of $\pm \text{sgn}(J)(A - B)$. Now recall that $T_c = \pm \text{sgn}(J) [A/B(T_c)] T_c^{\text{eq}}$ is larger than T_c^{eq} for the non-trivial magnetization to be well defined; therefore $\pm \text{sgn}(J) A > B$. Thus, $\pm \text{sgn}(J)(A - B) > B[1 \mp \text{sgn}(J)] \geq 0$. Hence, we conclude that the sign of $1 \mp C(\bar{\varphi})$ is positive and the solutions we found are stable.

Appendix B: Non-equilibrium steady-state Monte-Carlo

The results presented in this Letter are strictly exact in the limit of infinite coordination number (infinite dimensions). To check that these are not artifacts of the

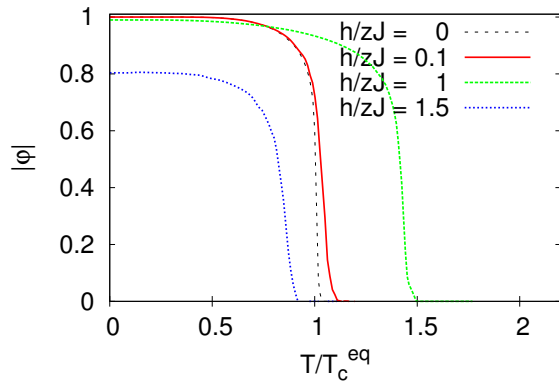


Figure 4: (color online) 2d Monte Carlo results of the magnetization $|\phi|$ as a function of the temperature T of the bath (super-Ohmic case, $s = 1$) at $\omega = zJ$ ($z = 4$) and for different values of the drive h given in the key ($L = 200$). Here $T_c^c = 2.2691J$ is the well known exact 2d critical temperature.

mean-field approximation, we computed exact numerical solutions by means of the Monte-Carlo algorithm that we adapted to non-equilibrium steady states. In finite dimension, once the steady state is reached, the rate at which spins are flipped are still given by Eq. (11), but now with $\epsilon_{\uparrow} = -J(n_{\uparrow} - n_{\downarrow}) = -\epsilon_{\downarrow}$ where n_{\uparrow} (n_{\downarrow}) is the number of spin up (down) neighbors. In practice, we initialize the lattice with a random spin configuration and update the configuration by randomly selecting spins and flipping them with probabilities governed by Eq. (11). Once a steady-state is reached, we measure the averaged magnetization in the lattice. We then repeat this procedure with different temperatures and drive strengths.

In Fig. 4, we present the results of such computations on a $2d$ lattice of size $L \times L$ with $L = 200$ that were averaged over 100 realizations of the non-thermal noise. The bath was taken to be super-Ohmic with simply $\nu(\epsilon) \propto \epsilon^{1+s}$ and $s = 1$. Note that the main qualitative features (*i.e.* the change of critical temperature, its trend as a function of h , and the decrease of the zero-temperature magnetization as a function of h) compare very well with the mean-field results presented in Fig. 1 of the Letter. The precise value of T_c as well as the critical behavior, $|\phi| \sim (T_c - T)^s$, cannot be accessed reliably within this numerical approach because of the finite-size effects that alter the small values of magnetization.

[1] A. J. Bray, Adv. Phys. **51**, 481 (2002).
[2] J. J. Arenzon, A. J. Bray, L. F. Cugliandolo, A. Sicilia, Phys. Rev. B **98**, 145701 (2008).
[3] J. Dziarmaga, Phys. Rev. B **74**, 064416 (2006).
[4] A. Sicilia, J. J. Arenzon, Alan J. Bray, L. F. Cugliandolo, EPL **82**, 10001 (2008).

[5] C. Aron, C. Chamon, L. F. Cugliandolo, M. Picco, J. Stat. Mech. P05016 (2008).
[6] S. Kohler, T. Dittrich, and P. Hanggi, Phys. Rev. E **55**, 300 (1997).
[7] D. W. Hone, R. Ketzmerick, and W. Kohn, Phys. Rev. E **79**, 051129 (2009).
[8] P. A. Rikvold, H. Tomita, S. Miyashita, and S. W. Sides, Phys. Rev. E **49**, 5080 (1994).
[9] R. A. Ramos, P. A. Rikvold, and M. A. Novotny, Phys. Rev. B **59**, 9053 (1999).
[10] F. Berthier, B. Legrand, J. Creuze and R. Tetot, J. Electroanal. Chem. **561**, 37 (2004).
[11] F. Berthier, B. Legrand, J. Creuze and R. Tetot, J. Electroanal. Chem. **562**, 127 (2004).
[12] S. Frank, D. E. Roberts and P. A. Rikvold, J. Chem. Phys. **122**, 064705 (2005).
[13] S. Frank and P. A. Rikvold, Surf. Sci. **600**, 2470 (2006).
[14] B. K. Chakrabarti and M. Acharyya, Rev. Mod. Phys. **71**, 847 (1999).
[15] S. W. Sides, P. A. Rikvold and M. A. Novotny, Phys. Rev. Lett. **81**, 834 (1998).
[16] S. W. Sides, P. A. Rikvold, and M. A. Novotny, Phys. Rev. E **59**, 2710 (1999).
[17] G. Korniss, C. J. White, P. A. Rikvold, and M. A. Novotny, Phys. Rev. E **63**, 016120 (2000).
[18] H. L. Richards, S. W. Sides, M. A. Novotny, and P. A. Rikvold, J. Magn. Magn. Mater. **150**, 37 (1995).
[19] M. A. Novotny, G. Brown, and P. A. Rikvold, J. Appl. Phys. **91**, 6908 (2002).
[20] Loic Herniet and Karyn Le Hur arXiv 1502.06863
[21] T. Tome and M. J. de Oliveira, Phys. Rev. A **41**, 4251 (1990).
[22] J. F. F. Mendes and E. J. S. Lage, J. Stat. Phys. **64**, 653 (1991).
[23] M. F. Zimmer, Phys. Rev. E **47**, 3950 (1993).
[24] G. M. Buendia and E. Machado, Phys. Rev. E **58**, 1260 (1998).
[25] M. Acharyya and B. K. Chakrabarti, Phys. Rev. B **52**, 6550 (1995).
[26] B. Chakrabarti and M. Acharyya, Rev. Mod. Phys. **71**, 847 (1999).
[27] W. S. Lo and R. A. Pelcovits, Phys. Rev. A **42**, 7471 (1990).
[28] G. Korniss, P. A. Rikvold and M. A. Novotny, Phys. Rev. E **66**, 056127 (2002).
[29] D. T. Robb, P. A. Rikvold, A. Berger and M. A. Novotny, Phys. Rev. E **76**, 021124 (2007).
[30] H. Fujisaka, H. Tutu and P. A. Rikvold, Phys. Rev. E **63**, 036109 (2001); 63, 059903(E) (2001).
[31] H. Tutu and N. Fujiwara, J. Phys. Soc. Jpn. **73**, 2680 (2004).
[32] E. Z. Meilikhov, JETP Lett. **79**, 620 (2004).
[33] S. B. Dutta, Phys. Rev. E **69**, 066115 (2004).
[34] D. T. Robb, Y. H. Xu, A. Hellwig, J. McCord, A. Berger, M. A. Novotny and P. A. Rikvold, Phys. Rev. B **78**, 134422 (2008).
[35] M. Bukov, L. D'Alessio, A. Polkovnikov, arXiv:1407.4803 (2014).
[36] L. M. Duan, E. Demler and M. D. Lukin, Phys. Rev. Lett. **91**, 090402 (2003).
[37] M. Greiner, O. Mandel, T. Esslinger, T. W. Hansch and I. Bloch, Nature **415**, 39 (2002).
[38] M. J. Hartmann, F. G. S. L. Brandao and M. B. Plenio, Laser & Photon. Rev. **2**, 527 (2008).